

## UNDERSTANDING DUAL AGN ACTIVATION IN THE NEARBY UNIVERSE

MICHAEL KOSS<sup>1,2</sup>, RICHARD MUSHOTZKY<sup>2</sup>, EZEQUIEL TREISTER<sup>3</sup>, SYLVAIN VEILLEUX<sup>2</sup>, RANJAN VASUDEVAN<sup>2</sup>, AND MARGARET TRIPPE<sup>2</sup>

*Draft version June 26, 2018*

### ABSTRACT

We study the fraction of dual AGN in a sample of 167 nearby ( $z < 0.05$ ), moderate luminosity, ultra hard X-ray selected AGN from the all-sky *Swift* BAT survey. Combining new *Chandra* and Gemini observations together with optical and X-ray observations, we find that the dual AGN frequency at scales  $< 100$  kpc is  $\sim 10\%$  (16/167). Of the 16 dual AGN, only 3 (19%) were detected using X-ray spectroscopy and were not detected using emission line diagnostics. Close dual AGN ( $< 30$  kpc) tend to be more common among the most X-ray luminous systems. In dual AGN, the X-ray luminosity of both AGN increases strongly with decreasing galaxy separation, suggesting that the merging event is key in powering both AGN. 50% of the AGN with a very close companion ( $< 15$  kpc), are dual AGN. We also find that dual AGN are more likely to occur in major mergers and tend to avoid absorption line galaxies with elliptical morphologies. Finally, we find SDSS Seyferts are much less likely than BAT AGN (0.25% vs. 7.8%) to be found in dual AGN at scales  $< 30$  kpc because of a smaller number of companions galaxies, fiber collision limits, a tendency for AGN at small separations to be detected only in X-rays, and a higher fraction of dual AGN companions with increasing AGN luminosity.

*Subject headings:* galaxies: active

### 1. INTRODUCTION

The detection and frequency of dual active galactic nuclei (AGN) on kpc scales is an important test of the merger-driven AGN model. Understanding the types of galaxies and specific merger stages where dual AGN occur provides important clues about the peak black hole growth during the merging process. Over the last decade, several nearby dual AGN on kpc scales have been found serendipitously in interacting galaxies (Komossa et al. 2003; Koss et al. 2011a). In addition, higher redshift dual AGN systems have been discovered using high resolution integral field spectroscopy or radio observations (Fu et al. 2011b). Finding these duals is an important step, but a systematic study of dual AGN offers the best chance of understanding their frequency and the types of galaxies and interactions involved in their triggering.

Early studies of the dual AGN frequency at higher redshift ( $z > 0.15$ ) focused on quasar pairs but suffered from severe observational difficulties detecting close pairs. Djorgovski (1991) found a 2x quasar overabundance on  $< 100$  kpc scales based on normal galaxy clustering. Other early observations found a small fraction (0.1%) of quasar pairs with typical separations of 50 to 100 kpc suggesting that at least one AGN shuts off on scales  $< 30$  kpc (Mortlock et al. 1999). Recent studies using the SDSS suggested dual quasars peak at small  $< 50$  kpc scales with a small excess extending to 100s of kpc (Hennawi et al. 2006; Foreman et al. 2009). Other recent studies found the opposite result with only a small excess at  $< 35$  kpc (Myers et al. 2007). However, on close scales

$< 30$  kpc, these observations are complicated by gravitational lenses (Narayan & White 1988; Kochanek et al. 1999) as well as an inability to easily resolve each AGN in optical and X-ray observations.

Nearby galaxies are better suited for dual AGN studies since both the nuclear engine and the host galaxies can be resolved and studied down to separations of a few kpc. A large study of optical AGN pairs at  $z < 0.16$  using SDSS spectroscopy found that their fraction was  $\approx 1.5\%$  within 30 kpc (Liu et al. 2011) while their cumulative fraction increases linearly with separation. However, because of fiber collision limits this technique suffers from incompleteness at close scales. Furthermore, optical surveys are incomplete since X-ray and IR selected AGN are not always detected optically (Hickox et al. 2009; Koss et al. 2011a). Therefore, a study of nearby AGN using emission line diagnostics and X-ray observations provides the best chance of accurately measuring the dual AGN frequency.

In this letter, we determine the incidence of dual AGN in the local Universe by searching for multiple active nuclei from the Koss et al. (2011b) sample of ultra hard X-ray selected AGN. This sample is ideal since archival X-ray data from *SWIFT* XRT, *XMM*, or *Chandra* exist for the entire set of objects. The ultra hard X-rays also offer a reliable tracer of the bolometric luminosity of AGN since it is nearly unaffected by host galaxy contamination or obscuration, which strongly affects other selection techniques such as optical emission lines, infrared spectral analysis, or optical colors.

### 2. DATA AND ANALYSIS

We adopt  $\Omega_m = 0.3$ ,  $\Omega_\Lambda = 0.7$ , and  $H_0 = 70$  km s<sup>-1</sup> Mpc<sup>-1</sup> to determine distances.

#### 2.1. Samples

The BAT AGN sample consists of 167 nearby ( $z < 0.05$ ) ultra hard X-ray BAT-detected AGN from Koss et al.

koss@ifa.hawaii.edu

<sup>1</sup> Institute for Astronomy, University of Hawaii, Honolulu, HI, USA

<sup>2</sup> Astronomy Department, University of Maryland, College Park, MD, USA

<sup>3</sup> Departamento de Astronomía, Universidad de Concepción, Concepción, Chile

(2011b) catalog in the Northern sky ( $>-25^\circ$ ), with low Galactic extinction ( $E(B - V) < 0.5$ ). For each BAT AGN, we search the SDSS, 6DF, 2DF, and NED for apparent companions within 100 kpc with small radial velocity differences ( $< 300 \text{ km s}^{-1}$ ). For comparison, we use a sample of emission line selected type 2 Seyferts in the SDSS taken from the Garching catalog, which we refer to as *SDSS Seyferts*. We use the emission line diagnostics of Veilleux & Osterbrock (1987), revised by Kewley et al. (2006). We require each optical AGN to be classified as Seyfert using the  $[\text{O III}] \lambda 5007/\text{H}\beta$  vs.  $[\text{N II}] \lambda 6583/\text{H}\alpha$ ,  $[\text{S II}] \lambda \lambda 6717, 6731/\text{H}\alpha$ , and  $[\text{O I}] \lambda 6300/\text{H}\alpha$  diagnostics, as well as having a  $\text{S/N} > 10$  in all lines. We restricted our SDSS Seyferts to  $z < 0.07$  totaling 1988 Seyferts.

## 2.2. X-ray Data

To determine the AGN nature of the galaxy companions, we use X-ray data from *Chandra*, *XRT*, or *XMM*. Because of the difficulty identifying dual X-ray point sources at separations  $< 20''$  with *XMM* or *XRT*, we obtained *Chandra* observations (PI: Mushotzky, 12700910) for 11 BAT AGN with close companions ( $< 20''$ ). The *Chandra* exposure times ensured  $> 10$  photons for a source with  $10^{41} \text{ erg s}^{-1}$  and a column density of  $5 \times 10^{23} \text{ cm}^{-2}$ ; objects with lower column densities will have more counts.

To fit X-ray spectra we assumed a fixed Galactic photoelectric absorption (Kalberla et al. 2005), a floating photoelectric absorption component, and a power law ( $F \propto E^{-\Gamma+2}$ ). For source counts we use a  $1.5''$  (3 pixel) radius aperture in *Chandra*,  $6''$  (1.5 pixel) radius in *XMM*, and  $7.1''$  (3 pixel) radius in *XRT*. We apply aperture corrections based on the point spread function (PSF) at 1.5 keV. For sources with  $< 50$  counts, we use a fixed power law of  $\Gamma = 1.8$ . For sources without detections, we calculate 95% confidence limit Poisson statistics assuming  $\Gamma = 1.8$  and  $N_{\text{H}} = 10^{22} \text{ cm}^{-2}$ .

## 2.3. Emission Line Diagnostics and Optical Data

We use optical spectroscopy from the SDSS DR8 to search for dual AGN within 100 kpc. Because of the  $55''$  fiber collision limits in the SDSS, we observed 11 BAT AGN galaxies with Gemini. We observed both galaxy nuclei simultaneously using the B600-G5307 grating with a  $1''$  slit in the 4300–7300 Å wavelength range, for 37 minutes each. We follow Winter et al. (2010) for correcting Milky Way reddening, starlight continuum subtraction, and fitting AGN diagnostic lines. To correct our line ratios for extinction, we use the narrow Balmer line ratio ( $\text{H}\alpha/\text{H}\beta$ ) assuming an intrinsic ratio of 3.1 and the Cardelli et al. (1989) reddening curve.

To compute the ratio of stellar masses of the AGN host galaxy and its companion, we use *ugriz* photometry and follow Koss et al. (2011b). If the galaxy nuclei were too close to accurately measure stellar masses in multiple filters, we use the ratio of *i* band luminosity to determine stellar mass ratios or if unavailable, ratios of K band luminosity from 2MASS.

## 2.4. Dual AGN Classification

We classify a source as a dual AGN when the companion galaxy’s optical emission line diagnostics or X-ray data indicate an AGN. We require that at least two

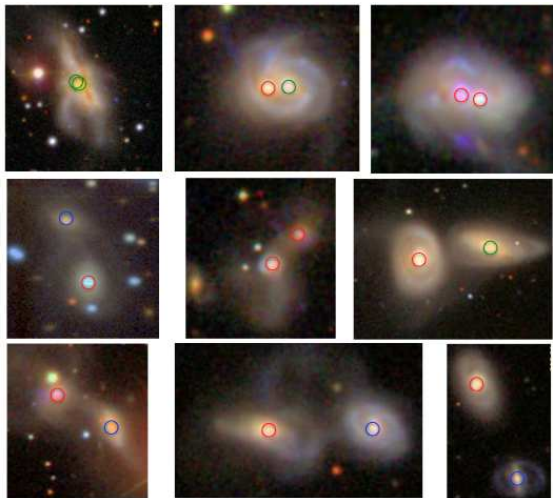


**Figure 1.** Nine composite *gri* images selected at random from 16 BAT detected dual AGN in Table 1. A red circle indicates X-ray and optical AGN detection. A green circle indicates X-ray AGN detection, but no optical detection. A blue circle indicates optical emission line diagnostics detect the AGN, but there are too few X-ray counts to detect an AGN.

of three emission line diagnostics indicate a Seyfert or LINER. For the companions of BAT detected AGN, we also use X-ray data for companion classification. Since X-rays can be produced from star formation, a galaxy is an AGN only if  $L_{2-10 \text{ keV}} > 10^{42} \text{ erg s}^{-1}$  or X-ray spectroscopy indicates a hard power law ( $\Gamma < 2$ ), an Fe K line, or rapid time variability indicative of an AGN. At  $L_{2-10 \text{ keV}} > 10^{42} \text{ erg s}^{-1}$ , a very high star formation rate ( $\text{SFR} > 200 M_{\odot} \text{ yr}^{-1}$ ) would be required to generate the observed hard X-ray luminosity (Ranalli et al. 2003). For AGN with multiple companions within 100 kpc, we test each galaxy pair separately and only compare the three nearest companions to ensure the sample is not dominated by galaxy groups. We note this AGN classification excludes some lower luminosity AGN with lower X-ray luminosities or composite optical spectra.

## 3. RESULTS

### 3.1. Companion Sample Study

We identify 81/167 (49%) of BAT AGN having at least one companion within 100 kpc. Additionally, 16 BAT AGN galaxies have two companions within 100 kpc and 5 have three or more companions within 100 kpc. The total number of companions in the sample is 106. A list of the BAT AGN and their companions can be found in Table 1. In the SDSS Seyfert sample, 358/1988 (18%) have at least one companion within 100 kpc. Additionally, 17 SDSS Seyferts have two companions within 100 kpc and 5 have three or more within 100 kpc, for a total of 385 companions.

We find that major mergers ( $M_1/M_2 < 3$ ) are more frequent at close separations for BAT and SDSS Seyferts. At  $< 15 \text{ kpc}$ , 78% (14/18) of BAT AGN galaxy companions have  $M_1/M_2 < 3$ , while at 60–100 kpc separations, only 30% (10/33) have  $M_1/M_2 < 3$ . Both the SDSS and BAT AGN sample show similar distributions of average stellar mass ratio with host galaxy separation. We also find that BAT AGN are more likely than SDSS Seyferts or inactive galaxies to have companions at small separations. Namely, at separations  $< 15 \text{ kpc}$ , 10% (16/167) of

BAT AGN have companions, while for the SDSS Seyferts this fraction is only 1% (20/1988), and only 2% (4/167) among inactive galaxies matched in stellar mass and redshift to the BAT AGN consistent with Koss et al. (2010).

### 3.2. Dual AGN Frequency with Projected Separation

Among the entire sample of BAT AGN and SDSS Seyferts, we find a lower limit of the dual AGN frequency between 1 and 100 kpc of 9.6% (16/167) for BAT AGN and 0.5% (10/1988) for SDSS Seyferts. These are lower limits because we exclude sources classified as composites by their optical emission line properties, and because both samples have incomplete X-ray and optical spectroscopy.

Sample images of the BAT detected dual AGN can be found in Figure 1. The majority of these dual AGN (75%, 12/16) are found on scales <30 kpc. NGC 835 is a triple AGN system with AGN companions at 15 and 87 kpc. A plot of the frequency of dual AGN by separation is in Figure 2. The dual AGN fraction peaks at small separations (<15 kpc), where 50% (8/16) are duals.

Dual AGN in the BAT and SDSS have, on average, smaller separations than the AGN with inactive companions. The mean and  $1\sigma$  values of the separations among BAT AGN and their companions are  $28\pm 24$  kpc, and  $50\pm 26$  kpc for the dual AGN and the AGN-inactive galaxy systems, respectively. A Kolmogorov-Smirnov (K-S) test indicates a negligible ( $<2\times 10^{-6}$ ) chance that the distribution of separations for the dual AGN and AGN-inactive systems are from the same distribution. A similar result is found for SDSS Seyferts with separations of  $41\pm 30$  kpc, and  $64\pm 24$  kpc for the dual AGN and single AGN systems, respectively, with a  $<5\%$  chance from a K-S test. The BAT AGN in duals are at smaller separations than SDSS Seyferts in duals with a  $<0.01\%$  chance of being from the same distribution.

### 3.3. Host Properties of Dual AGN

We studied the galaxy morphologies and merger types of systems hosting dual AGN. We limited this study to projected separations <30 kpc because of the low frequency of duals found at larger separations and the higher chance of projection effects causing the galaxies to appear to be at artificially small separations. We find that the frequency of dual AGN is strongly dependent on galaxy mass ratio (Figure 2) suggesting a minor merger is insufficient to trigger dual AGN. The mean stellar mass ratio and  $1\sigma$  are  $2.1\pm 1.3$ . The highest fraction of duals occurs in galaxy pairs with small stellar mass ratios ( $M_1/M_2 < 3$ ) where 65% (11/17) of these pairs are in dual. No dual AGN are found in galaxy pairs with  $M_1/M_2 > 6$ .

We also investigated the types of galaxies that are single AGN systems even though they have a close companion (<30 kpc) and a small stellar mass ratio (<6). This includes a total of 11 systems (Figure 3). In optical spectroscopy, five of these companion galaxies are red elliptical absorption line galaxies, two are star forming emission line galaxies, and four have no available optical spectroscopy. In the X-rays, 4/11 are at separations  $<20''$ , where a faint dual AGN may be missed and have no *Chandra* observations. The two star forming emission line galaxies not classified as duals are UGC 4727 and SDSS J112648.65+351454.2. UGC 4727 is at

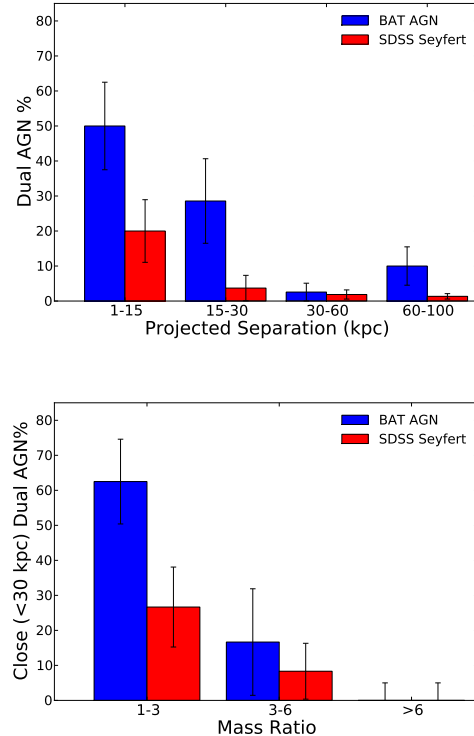


**Figure 2.** *Top:* frequency of dual AGN for galaxies with companions as a function of apparent separation. Error bars assume binomial statistics. We find the dual AGN frequency increases at smaller separations in BAT AGN and SDSS Seyferts. *Bottom:* frequency of dual AGN as a function of the ratio of galaxy stellar masses. We limited this study to projected separations <30 kpc because of the low frequency of duals found at larger separations. The dual AGN frequency increases in major mergers for both BAT AGN and SDSS Seyferts.

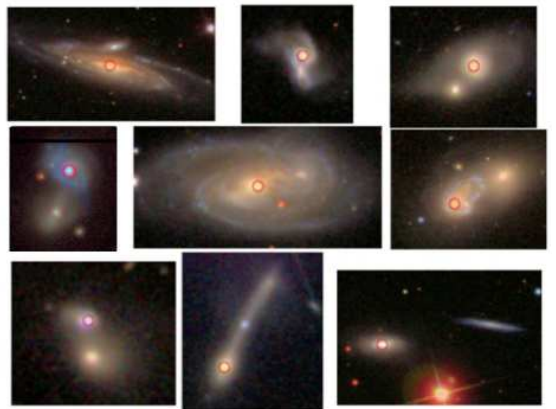


**Figure 3.** Composite *gri* filter images of nine BAT AGN hosts with inactive companions within 30 kpc. A red circle indicates the BAT AGN. We find the majority of inactive companions are elliptical absorption line galaxies or minor mergers.

stellar mass 5.9 times lower than the BAT source and a separation of 26 kpc. UGC 4727 is also a bulgeless galaxy. The other galaxy with star forming emission line diagnostics is SDSS J112648.65+351454.2 with a stellar mass 3.6 times lower than the BAT AGN, Mrk 423. These results suggest that dual AGN tend to avoid elliptical/absorption line galaxies.

### 3.4. X-ray Properties of BAT AGN in Duals

We detect 12/16 of the dual AGN using X-rays. Four of the secondary AGN are detected using optical spectroscopy, but have no X-ray detection. One of these, UGC 11185, has a large upper limit because of its close proximity ( $28''$ ) to a bright BAT AGN. The remaining dual AGN with X-ray non-detections are at large separations ( $>40$  kpc) and have a lower stellar mass than the BAT AGN ( $M_2/M_1 > 3$ ). The median value of the  $L_{2-10 \text{ keV}}$  ratio between the dual AGN is 11, but varies dramatically, with the smallest ratio being 1.1 between NGC 6240S and NGC 6240N, and some dual pairs having X-ray ratios greater than 1000 (IRAS 05589+2828 and UGC 8327).

We find that the X-ray luminosity of both AGN increases with decreasing separation, suggesting that the merging event is key to powering both AGN (Figure 4). For example, the six most luminous companion AGN are found at small separations ( $<15$  kpc). A Spearman correlation test indicates a  $>99.998\%$  probability that the  $L_{2-10 \text{ keV}}$  of the AGN companion and separation are inversely correlated. Similarly, a Spearman test indicates a  $>90\%$  that the primary AGN 2-10 keV luminosity and separation are inversely correlated. Finally, a Spearman test indicates a  $>98.8\%$  chance the ultra hard X-ray luminosity is inversely correlated with separation, however, this low spatial resolution measure may be biased towards small separations because it includes emission from both AGN.

Finally, we investigated the close ( $<30$  kpc) dual AGN fraction with bolometric luminosity assuming a conversion factor of  $L_{\text{bol}} = 15 \times L_{14-195 \text{ keV}}$  based on Vasudevan et al. (2010). For systems with  $L_{\text{bol}} > 10^{45} \text{ erg s}^{-1}$ , the mean bolometric luminosity is  $(2.2 \pm 1.1) \times 10^{45} \text{ erg s}^{-1}$  and 17.1% (6/35) are close ( $<30$  kpc) dual AGN. Among less luminous systems, the mean bolometric luminosity is  $(4.4 \pm 2.9) \times 10^{44} \text{ erg s}^{-1}$  and dual fraction is 4.5% (6/132). This suggests that close dual AGN may be more common among luminous systems.

## 4. SUMMARY AND DISCUSSION

We study the frequency of dual AGN in nearby ultra hard X-ray selected BAT AGN using archival optical and X-ray imaging spectroscopy along with new observations from Gemini and *Chandra*. We find:

- (i) Dual AGN are much more likely to occur in systems with a close companion within  $<30$  kpc among BAT AGN and SDSS Seyferts. Among BAT AGN with a companion at small separations ( $<15$  kpc), a high fraction (50%, 8/16) are duals.
- (ii) In 19% (3/16) of the dual AGN in the BAT sample, X-ray spectroscopy reveals the presence of a dual AGN that is not detected with emission line diagnostics (NGC 6240, Mrk 739, NGC 833).
- (iii) The hard X-ray luminosities of both AGN increase as the separation between the galaxies decrease suggesting that the merging event is key in powering the AGN. Additionally, close dual AGN ( $<30$  kpc) tend to be more common among the most X-ray luminous systems with  $L_{\text{bol}} > 10^{45} \text{ erg s}^{-1}$ . This is in agreement with recent simulations suggesting

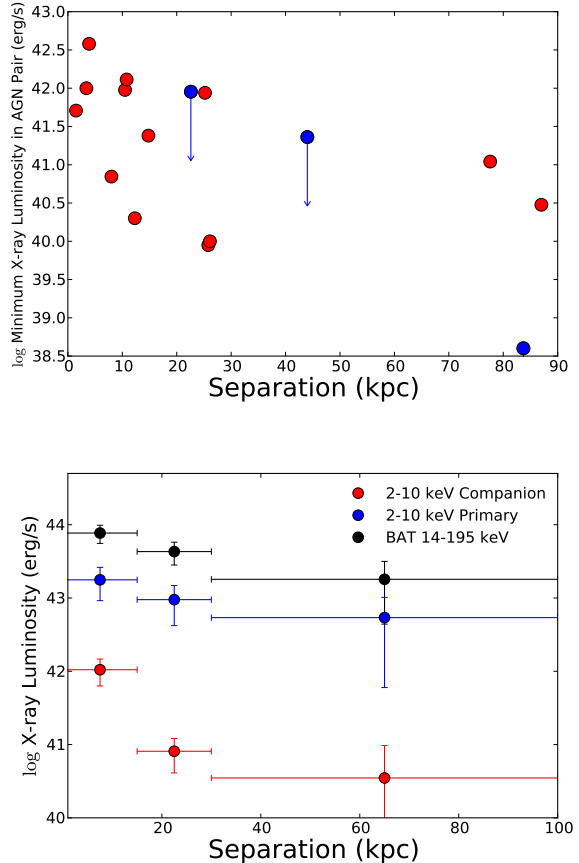


**Figure 4.** *Top:* plot of minimum  $L_{2-10 \text{ keV}}$  in 16 dual AGN pairs by galaxy separation. Blue points are upper limits. *Bottom:* binned average of X-ray luminosity with separation. The X-ray luminosity of the primary and secondary AGN increases towards smaller separations.

the peak accretion and BH luminosity appear at small scales while relatively lower luminosity dual AGN are found at wider separations (Van Wassenhove et al. 2011).

- (iv) Dual AGN are more prominent among major mergers ( $M_1/M_2 < 3$ ) and avoid absorption line galaxies with elliptical morphologies. However, AGN activity is more difficult to detect in dwarf companions because of the likely lower mass BHs.
- (v) We find SDSS Seyferts are much less likely than BAT AGN (0.25% vs. 7.8%) to be found in dual AGN at scales  $<30$  kpc.

These results suggest that in systems already hosting a single AGN, nuclear activity in companions is triggered in the majority of close-separation major mergers. *Indeed, our sample finds that all 11 BAT AGN with non-absorption line companions in major mergers ( $M_1/M_2 < 3$ ) and close separations ( $<30$  kpc) are dual AGN.* Our sample also suggests that early-type gas-poor (red/elliptical) companions are unlikely to host AGN, possibly because it may not be able to capture enough gas during the merging process. From these results, one might expect a high dual AGN fraction in luminous infrared galaxies (LIRGs) which are associated with gas-

rich mergers. However, only a few dual AGN in this sample are LIRGs (e.g., NGC 6420, Mrk 463) which is consistent with the overall fraction of LIRGs in the rest of the BAT sample (18%, Koss et al. 2010). Therefore, it seems that the particular type of merger triggering the luminous BAT AGN also triggers the secondary AGN.

Dual AGN systems are more common in ultra hard X-ray selected AGN than SDSS Seyferts since they have more close companions (Koss et al. 2010). Since there are more dual AGN among BAT AGN than SDSS Seyferts by more than a factor of 10, the much higher fraction is most likely mainly because of the higher AGN luminosities of BAT AGN, not the lack of X-ray observations of SDSS Seyferts.

We also find a higher total fraction of dual AGN compared to dual AGN studies using the double peaked method (Comerford et al. 2009). At scales  $<15$  kpc, we find 5% (8/167) are dual AGN,  $\approx 10$ x higher than that estimated from double peak sources (0.3-0.5%, at  $z \approx 0.4$ , Rosario et al. 2011,  $< 3\%$ , at  $z \approx 0.1-0.6$ , Fu et al. 2011). This is likely because: 1) double peak sources are at higher redshifts,  $\approx 10$  times that of this sample ( $z=0.02$  vs.  $z=0.3$ ) so they are more difficult to detect as dual AGN, 2) the SDSS fiber is  $3''$ , so it is sensitive to different, typically smaller physical scales (at  $z = 0.4$ ,  $3'' \approx 15$  kpc), 3) the double peak method is biased towards selecting certain types of single AGN such as radio bright AGN (Smith et al. 2010), which is different than BAT AGN where only 0.5% are radio loud (Teng et al. 2011), 4) the double peak method has difficulty detecting dual AGN with small velocity offsets, weak lines, or those dual AGN that are detected only in the X-rays like NGC 6240. Finally, because of the fixed SDSS fiber size, the double peak method is sensitive to AGN with different physical separations and different luminosities depending on the redshift range studied making a comparison difficult, but our results suggest that the fraction of dual AGN is much higher than the double peak method suggests among luminous AGN.

This type of extensive study is impossible to do at higher redshifts because of surface brightness dimming and the limitations in resolution and exposure time, particularly in X-rays since the secondary AGN are typically 10-100x fainter. However, the pair fraction and frequency of gas-rich "wet" galaxy mergers increases with redshift. This suggests that dual AGN activation may be much more common at higher redshifts.

## REFERENCES

- Cardelli, J. A., Clayton, G. C., & Mathis, J. S. 1989, ApJ, 345, 245
- Comerford, J. M., et al. 2009, ApJ, 698, 956
- de Carvalho, R. R., & Coziol, R. 1999, AJ, 117, 1657
- Djorgovski, S. 1991, ASP Conference Series, 21, 349
- Foreman, G., Volonteri, M., & Dotti, M. 2009, ApJ, 693, 1554
- Fu, H., Myers, A. D., Djorgovski, S. G., & Yan, L. 2011a, ApJ, 733, 103
- Fu, H., et al. 2011b, eprint arXiv, 1109, 8
- Hennawi, J. F., et al. 2006, AJ, 131, 1
- Hickox, R. C., et al. 2009, ApJ, 696, 891
- Ho, L. C., Filippenko, A. V., Sargent, W. L. W., & Peng, C. Y. 1997, ApJS, 112, 391
- Kalberla, P. M. W., Burton, W. B., Hartmann, D., Arnal, E. M., Bajaja, E., Morras, R., & Pöppel, W. G. L. 2005, A&A, 440, 775
- Kewley, L. J., Groves, B., Kauffmann, G., & Heckman, T. 2006, MNRAS, 372, 961
- Kochanek, C. S., Falco, E. E., & Muñoz, J. A. 1999, ApJ, 510, 590
- Komossa, S., Burwitz, V., Hasinger, G., Predehl, P., Kaastra, J. S., & Ikebe, Y. 2003, ApJ, 582, L15
- Koss, M., et al. 2011a, ApJL, 735, L42
- Koss, M., Mushotzky, R., Veilleux, S., & Winter, L. 2010, ApJL, 716, L125
- Koss, M., Mushotzky, R., Veilleux, S., Winter, L. M., Baumgartner, W., Tueller, J., Gehrels, N., & Valencic, L. 2011b, ApJ, 739, 57
- Liu, X., Shen, Y., Strauss, M. A., & Hao, L. 2011, ApJ, 737, 101
- Mortlock, D. J., Webster, R. L., & Francis, P. J. 1999, Monthly Notices, 309, 836
- Myers, A. D., Brunner, R. J., Richards, G. T., Nichol, R. C., Schneider, D. P., & Bahcall, N. A. 2007, ApJ, 658, 99
- Narayan, R., & White, S. D. M. 1988, Royal Astronomical Society, 231, 97P
- Ranalli, P., Comastri, A., & Setti, G. 2003, A&A, 399, 39
- Rosario, D. J., McGurk, R. C., Max, C. E., Shields, G. A., Smith, K. L., & Ammons, S. M. 2011, ApJ, 739, 44
- Smith, K. L., Shields, G. A., Bonning, E. W., McMullen, C. C., Rosario, D. J., & Salvander, S. 2010, ApJ, 716, 866
- Teng, S. H., Mushotzky, R. F., Sambruna, R. M., Davis, D. S., & Reynolds, C. S. 2011, ApJ, 742, 66
- Vasudevan, R. V., Fabian, A. C., Gandhi, P., Winter, L. M., & Mushotzky, R. F. 2010, MNRAS, 402, 1081
- Veilleux, S., Kim, D.-C., Sanders, D. B., Mazzarella, J. M., & Soifer, B. T. 1995, Astrophysical Journal Supplement v.98, 98, 171
- Veilleux, S., & Osterbrock, D. E. 1987, ApJSS, 63, 295
- Winter, L. M., Lewis, K. T., Koss, M., Veilleux, S., Keeney, B., & Mushotzky, R. F. 2010, ApJ, 710, 503

Table 1 Dual AGN Study of BAT Sample

BAT Source Name	Galaxy Comp. <sup>1</sup>	Sep kpc	$M_1/M_2$ <sup>2</sup>	X-ray 2 <sup>3</sup> 2-10 keV	Opt 2 <sup>4</sup> Diag	Refs <sup>5</sup> X-ray	Refs <sup>6</sup> Opt
<i>Dual AGN Systems</i>							
NGC 6240S	NGC 6240N	1.5	1.6	0.51	? / ?	CXO	
Mrk 739E	Mrk 739W	3.4	0.5	1	C/SF/SF	CXO	G
Mrk 463E	Mrk 463W	3.9	1.2	3.8	AGN/Sy2/Sy2	CXO	S
IRAS 05589+2828	2MASX J06021107+2828382	8	5.7	0.07	AGN/Sy2/Sy2	CXO	G
ESO 509-IG 066 NED 02	ESO 509-IG066E	10.5	1.6	0.95	AGN/Sy2/Sy2	XMM	6DF
IRAS 03219+4031	2MASX J03251221+4042021	10.8	2.6	1.3	AGN/Sy2/Sy2	XMM	4
NGC 3227	NGC 3226	12.3	1.7	0.02	AGN/L/L	CXO	1
NGC 835	NGC 833	14.8	1.5	0.7	SF/L/SF	XMM	S
UGC 11185 NED02	UGC 11185 NED01	22.6	1.3	$< 0.9$	AGN/Sy2/Sy2	XRT	G
MCG +04-48-002	NGC 6921	25.2	0.4	0.87	Sy2	XMM	N
NGC 2992	NGC 2993	25.8	2.7	0.0089	SF/SF/SF	XMM	6DF
UGC 8327 NED02	UGC 8327 NED01	26.1	2.8	0.014	AGN/Sy2/Sy2	CXO	S

Continued on Next Page...

TABLE 1 – Continued

BAT Source Name	Galaxy Comp. <sup>1</sup>	Sep kpc	$M_1/M_2^2$	X-ray 2 <sup>3</sup> 2-10 keV	Opt 2 <sup>4</sup> Diag	Refs <sup>5</sup> X-ray	Refs <sup>6</sup> Opt
Mrk 268	MRK 268SE	44	5.5	< 0.23	AGN/Sy2/Sy2	XMM	S
NGC 7679	NGC 7682	77.6	2.3	0.11	Sy2	XMM	5
NGC 1052	NGC 1042	83.7	3.3	< 0.0004	C/SF/Sy2	CXO	S
M106	NGC 4220	85.7	12	?	AGN/Sy2/Sy2		1
NGC 835	NGC 839	87	2.1	0.03	AGN/Sy2/?	XMM	6
<i>Single AGN Systems</i>							
Mrk 423	SDSS J112648.65+351454.2	5.9	3.6	< 1.8	SF/SF/SF	XRT	S
NGC 931	LEDA 212995	6	6.1	< 0.0076	HII	CXO	3
ARP 151	SDSS J112535.23+542314.3	8.2	1.4	< 0.33	Abs	XRT	S
2MASX J09043699+5536025	2MASX J09043675+5535515	9	0.9	< 9.3	Abs	XMM	G
NGC 235A	NGC 235B	9	5.5	< 0.011	Abs	CXO	G
UGC 03995	UGC 03995A	10.3	8.2	< 0.0086	SF/SF/SF	CXO	S
2MASX J11454045-1827149	2MASX J11454080-1827359	14	1.2	0.04	Abs	CXO	G
NGC 3786	NGC 3788	14	1.2	< 0.015	?	XMM	
FAIRALL 0272		19	15.6	< 0.038	?	XMM	G
Mrk 348	2MASX J00485285+3157309	22	5.2	0.0091	?	XMM	
KUG 1208+386	2MASX J12104784+3820393	24.1	11	< 0.17	SF/SF/SF	XMM	S
NGC 5106	PGC 046603	25	6.6	< 0.046	SF/SF/SF	XRT	S
NGC 7469	IC 5283	25	4.5	< 0.0017	?	CXO	
UGC 05881	SDSS J104644.87+255502.1	25.1	20.9	< 0.0072	SF/SF/SF	XRT	S
Mrk 18	UGC 04727	25.9	5.9	< 0.037	SF/SF/SF	XMM	S
NGC 1142	NGC 1143	26	1.7	< 0.045	Abs	XMM	S
Mrk 279	MCG +12-13-024	27	7.5	< 0.2	?	XMM	G
NGC 5506	NGC 5507	27.2	2.3	< 0.00085	Abs	XMM	6DF
UGC 07064	SDSS J120445.20+311132.9	30.3	5.2	< 0.019	Abs	XMM	S
MCG +06-24-008	SDSS J104444.22+381032.9	30.7	33.9	< 0.077	LowSN	XRT	S
NGC 3079	CGCG 265-055	30.9	47.9	0.0016	SF/SF/SF	XMM	S
UGC 07064	2MASX J12044518+3111327	31	6.7	< 0.014	?	XMM	
MCG -01-24-012	MCG -01-24-011	32.5	0.9	< 0.18	Abs	XMM	6DF
MCG -02-12-050	2MASX J04381113-1047474	33	5.1	< 0.4	?	XRT	
Mrk 590	SDSS J021429.36-004604.7	33.8	34.7	0.007	Abs	XMM	S
UGC 06527 NED03	UGC 06527 NOTES02	35.7	0.5	< 0.022	SF/SF/SF	XMM	S
FAIRALL 272	Fairall 0273	36	4.8	0.026	?	XMM	
NGC 5231	SDSS J133542.77+030006.7	36.3	25.7	< 0.017	SF/SF/SF	XMM	S
MCG -01-13-025	2MASX J04514177-0350295	36.8	5	< 0.050	abs	XMM	6DF
UGC 07064	SDSS J120445.27+310927.8	36.9	5.5	0.051	SF/SF/SF	XMM	S
LEDA 214543	NGC 6230 NED02	38.5	0.6	< 0.053	?	XRT	
Mrk 477	PGC 052445	39	1.6	?	?		
2MASX J09043699+5536025	2MASX J09043156+5535326	41	0.9	< 0.64	?	XMM	
NGC 7319	NGC 7318A	41	0.7	0.019	?	CXO	
NGC 4593	MCG -01-32-033	41.1	58.9	< 0.00097	SF/SF/?	XMM	6DF
UGC 06527 NED03	UGC 06527 NOTES01	41.8	2.6	< 0.011	SF/SF/SF	XMM	S
Mrk 268	2MASX J13411364+3023281	44.2	27.5	< 0.071	SF/SF/SF	XMM	S
NGC 1194	2MASX J03034116-0104249	44.2	4.2	< 0.0037	SF/SF/SF	XMM	S
NGC 513	KUG 0121+335	44.6	9.3	< 0.033	?	XMM	
NGC 3079	NGC 3073	45	25.7	< 0.0021	SF/SF/SF	CXO	1
NGC 2992	FGC 0938	45.5	90.8	< 0.013	?	XMM	
SBS 0915+556	2MASX J09191393+5528422	47	0.7	< 0.2	SF/SF/SF	XRT	S
NGC 3718	NGC 3729	47.7	2.4	0.0025	?	CXO	
2MASX J09112999+4528060	SDSS J091122.60+452717.2	49	9.1	< 0.0063	SF/SF/SF	XMM	S
NGC 4388	VPC 0415	49.2	134.9	< 0.017	LowSN	XMM	S
NGC 5290	SDSS J134529.67+413831.0	49.4	134.9	< 0.004	LowSN	XRT	S
NGC 2885	UGC 05037 NOTES02	52.9	4	< 0.051	Abs	XRT	S
NGC 235A	NGC 0232	53.8	0.8	0.11	AGN/SF/SF	CXO	6DF
NGC 3081	TOLOLO 0957-225	54	?	< 0.0025	?	XRT	
NGC 1052	2MASX J02413514-0810243	54.8	56.2	< 0.00036	Abs	CXO	S
NGC 5252	SDSS J133811.34+043052.4	54.8	61.7	< 0.036	SF	XMM	S
NGC 2885	MCG +04-22-060	56.2	3.3	< 0.052	Abs	XRT	S
NGC 835	NGC 838	56.7	2.3	< 0.05	SF/SF/SF	XMM	S
Mrk 926	2MASX J23044397-0842114	58.7	3.3	< 0.56	Abs	XMM	S
MCG -02-12-050	2MASX J04381880-1047004	58.9	9.4	< 0.15	?	XRT	
Mrk 915	MCG -02-57-024	59.6	11.8	< 0.02	?	XRT	
SBS 1301+540	MCG +09-21-095	60	6.2	< 0.035	SF/SF/SF	XMM	S
NGC 5290	SDSS J134548.55+414443.5	61.7	107.2	< 0.018	LowSN	XRT	S
NGC 1052	NGC 1047	62.4	22.4	< 0.00055	Abs	XMM	S
MCG -01-24-012	MCG -01-24-013	63.6	2.1	< 0.2	SF/SF/SF	XMM	6DF
NGC 1142	2MASX J02550661-0009448	66.6	7.5	< 0.045	Abs	XMM	S
KUG 1141+371	SDSS J114435.26+365408.8	66.9	12.3	< 0.14	SF/SF/SF	XMM	S
M106	NGC 4217	67	6.3	< 0.0001	Comp/SF/SF	CXO	1
Mrk 464	SDSS J135550.25+383332.0	67.7	2.1	< 0.034	SF/SF/SF	XMM	S
2MASX J07595347+2323241	SDSS J075959.87+232448.2	69	23.4	< 0.27	SF/SF/SF	XMM	S
Mrk 1469	SDSS J121617.69+505020.4	69.2	13.2	< 0.063	SF/SF/SF	XRT	S
Mrk 477	2MASX J14403849+5328414	71.2	5	?	SF/SF/SF	XRT	S
IC 0486	SDSS J080013.23+263525.2	72.8	32.4	< 0.050	SF/SF/SF	XRT	S
NGC 3079	SDSS J100331.69+553121.1	75.7	151.4	?	SF/SF/SF	XRT	S

Continued on Next Page. . .

TABLE 1 – Continued

BAT Source Name	Galaxy Comp. <sup>1</sup>	Sep kpc	$M_1/M_2$ <sup>2</sup>	X-ray 2 <sup>3</sup> 2-10 keV	Opt 2 <sup>4</sup> Diag	Refs <sup>5</sup> X-ray	Refs <sup>6</sup> Opt
UM 614	2dFGRS N404Z023	77.7	?	< 0.61	SF/Sy/?	XMM	2DF
NGC 4388	VCC 0871	79.5	42.7	< 0.19	LowSN	XMM	S
NGC 7319	NGC 7317	80.9	1.6	0.011	?	CXO	
2MASX J11454045-1827149	1H 1142-178:[KPC2006] 2	82.9	?	< 0.038	?	CXO	
Mrk 817	2MASX J14362084+5845279	83.1	4.1	< 0.34	SF/SF/SF	XMM	S
MCG +02-21-013	SDSS J080440.36+104513.0	83.4	47.9	< 0.07	SF/SF/LowSN	XRT	S
Mrk 352	CGCG 501-056	85.6	2.1	< 0.008	?	XMM	
NGC 973	IC 1815	88.6	2.2	< 0.034	?	XRT	
Mrk 1392	CGCG 048-116	88.7	1	< 0.31	?	XRT	
NGC 4686	SDSS J124609.71+543144.8	89.6	136	< 0.0048	SF/SF/SF	XMM	S
ARK 347	SDSS J120425.69+201548.9	89.9	6.3	< 0.031	Abs	XRT	S
CGCG 319-007	MCG +11-19-005	94.5	2.2	< 0.1	?	XRT	
Mrk 704	SDSS J091832.18+161604.0	94.8	55	< 0.07	SF/SF/SF	XRT	S
NGC 4619	SDSS J124134.51+350634.6	97.4	100	?	SF/SF/SF		S
NGC 5899	NGC 5900	98.7	2.2	< 0.0004	?	XMM	
UGC 03995	SDSS J074349.16+291154.5	99	36.9	< 0.01	Abs	CXO	S
NGC 973	2MFGC 02027	99.1	19.3	?	?		

<sup>1</sup> Projected separation.<sup>2</sup> Host galaxy stellar mass ratio between BAT AGN and companion.<sup>3</sup> Galaxy companion  $L_{2-10\text{ keV}}$  in units of  $10^{42}\text{ erg s}^{-1}$ .<sup>4</sup> AGN diagnostics from [O III]  $\lambda 5007/H\beta$  vs. [N II]  $\lambda 6583/H\alpha$ , [S II]  $\lambda\lambda 6717, 6731/H\alpha$ , and [O I]  $\lambda 6300/H\alpha$  ratios.<sup>5</sup> CXO=*Chandra*, XRT=*Swift*.<sup>6</sup> Optical spectroscopy where S=SDSS, G=Gemini, N=NED, 1=Ho et al. (1997), 2=Winter et al. (2010), 3=Veilleux & Osterbrock (1987), 4=Trippé in prep, 5=Veilleux et al. (1995), 6=de Carvalho & Coziol (1999)<sup>7</sup> ? indicates no available X-ray or optical spectroscopy for the companion.